



# Exploring the Relationship Between Time Series of Sentinel-1 Interferometric Coherence Data and Wild Edible Mushroom Yields in Mediterranean Forests

Raquel Martínez-Rodrigo<sup>1,2</sup> · Beatriz Águeda<sup>2,3</sup> · Juan M. Lopez-Sanchez<sup>4</sup> · José Miguel Altelaarrea<sup>1</sup> · Pablo Alejandro<sup>5,6,7</sup> · Cristina Gómez<sup>2,8</sup>

Accepted: 18 September 2024 / Published online: 8 November 2024  
© The Author(s) 2024

## Abstract

Edible wild mushrooms constitute a valuable marketable non-wood forest product with high relevance worldwide. There is growing interest in developing tools for estimation of mushroom yields and to evaluate the effects that global change may have on them. Remote sensing is a powerful technology for characterization of forest structure and condition, both essential factors in triggering mushroom production, together with meteo-climatic factors. In this work, we explore options to apply synthetic aperture radar (SAR) data from C-band Sentinel-1 to characterize, at the plot level, wild mushroom productive forests in the Mediterranean region, which provide saprotroph and ectomycorrhizal mushrooms. Seventeen permanent plots with mushroom yield data collected weekly during the productive season are characterized with dense time series of Sentinel-1 backscatter intensity (VV and VH polarizations) and 6-day interval interferometric VV coherence during the 2018–2021 period. Weekly-regularized series of SAR data are decomposed with a LOESS approach into trend, seasonality, and remainder. Trends are explored with the Theil-Sen test, and periodicity is characterized by the Discrete Fast Fourier transform. Seasonal patterns of SAR time-series are described and related to mycorrhizal and saprotroph guilds separately. Our results indicate that time series of interferometric coherence show cyclic patterns which might be related with annual mushroom yields and may constitute an indicator of triggering factors in mushroom production, whereas backscatter intensity is strongly correlated with precipitation, making noisy signals without a clear interpretable pattern. Exploring the potential of remotely sensed data for prediction and quantification of mushroom yields contributes to improve our understanding of fungal biological cycles and opens new ways to develop tools that improve its sustainable, efficient, and effective management.

**Keywords** SAR time series data · Non-wood forest products · Mediterranean forest

✉ Cristina Gómez  
cgomez@uva.es

Raquel Martínez-Rodrigo  
raquel.martinezrodrigo@cesefor.com

Beatriz Águeda  
beatriz.agueda@uva.es; beatriz.agueda@fora.es

Juan M. Lopez-Sanchez  
juanma.lopez@ua.es

José Miguel Altelaarrea  
josemiguel.altelaarrea@cesefor.com

Pablo Alejandro  
palejandro@quasarsr.com; pablo.alejandro@uva.es

<sup>3</sup> Föra Forest Technologies SLL, C/ de La Universidad S/N, 42004 Soria, Spain

<sup>4</sup> Institute for Computer Research, University of Alicante, 03080 Alicante, Spain

<sup>5</sup> Quasar Science Resources, Ctra. La Coruña Km 22.3, 28232 Las Rozas, Madrid, Spain

<sup>6</sup> Department of Applied Physics, Universidad de Valladolid, Campus Duques de Soria, 42004 Soria, Spain

<sup>7</sup> Department of Environment and Agroforestry, Catholic University of Avila, C/ Canteros S/N, 05005 Avila, Spain

<sup>8</sup> Department of Geography and Environment, School of Geoscience, University of Aberdeen, Aberdeen AB24 3UE, UK

<sup>1</sup> Fundación Cesefor, Calle C, 42005 Soria, Spain

<sup>2</sup> iuFOR, EiFAB, Universidad de Valladolid, Campus Duques de Soria, 42004 Soria, Spain

## Introduction

Predicting mushroom presence, occurrence, and productivity has growing interest (Küçüker and Başkent 2014; Herrero et al. 2019) as fungi provide a wide range of ecosystem services (Devkota et al. 2023) and contribute to maintain and augment biodiversity of other taxa (Müller and Bütler 2010; Cockle et al. 2012). The triggering factors in mushroom production are complex (Alday et al. 2017), being precipitation of paramount importance (Ágreda et al. 2015). Furthermore, mushroom development and productivity are strongly related with forest structure (Tomao et al. 2017), particularly with density and age (Ágreda et al. 2013; Martínez-Rodrigo et al. 2022).

## Remote Sensing in Forest Applications

Satellite remote sensing has become a major technology in environmental applications (Beland et al. 2019). Remote sensing is particularly well suited for the assessment of forest resources (White et al. 2016) and changes over time, thanks to its overall perspective and spatial completeness (Li and Roy 2017). The assessment of forest products, particularly wood (e.g., Eitel et al. (2020)) but also non-wood products like pine-nuts (e.g., Blázquez-Casado et al. (2019)), cork (e.g., Soares et al. (2022)), or mushrooms (e.g., Olano et al. (2020)) has been favored using remote sensing. While passive sensors from MODIS, Landsat or Sentinel-2 are widely employed, active sensors are increasingly being adopted for various applications (e.g., Ballère et al. (2021)). For instance, LiDAR is used to characterize forest structure (Dassot et al. 2011; Indirabai et al. 2019) and has shown potential to contribute in the estimation of mushroom yields in Mediterranean forests (Martínez-Rodrigo et al. 2022; Pascual and de-Miguel 2022).

## The Potential of SAR for Monitoring Mushroom Production

Synthetic aperture radar (SAR) is also an active-sensor technology that provides useful data in all atmospheric conditions (Pulella et al. 2020), and it is well-suited for characterization of forest structure (Neumann et al. 2010; Gómez et al. 2021). Moreover, the high frequency of data and open access policy of the Copernicus Sentinel-1 program (<https://scihub.copernicus.eu/>), together with improved data processing, have triggered new opportunities for application of SAR-based approaches in characterization of forests (Dostálová et al. 2018), mapping

of above-ground forest biomass (Cartus et al. 2022), and assessment of change (Tanase et al. 2019).

In the context of mushroom production, SAR can provide valuable insights due to its sensitivity to vegetation moisture and structure, which are critical factors influencing fungi development. The ability of SAR to penetrate forest canopies and provide consistent data under various weather conditions makes it an ideal tool for monitoring the environmental variables that affect mushroom growth over time.

## Time Series Analysis and SAR in Mushroom Growth Monitoring

Time series of radiometric data identify intra-annual vegetation patterns (Gómez et al. 2020) and anomalies (Rubio-Cuadrado et al. 2021). Since retrieving good quality time series of optical data without gaps becomes difficult in cloud-prone areas (Komisarenko et al. 2022), time series of SAR data are being explored for applications like seasonality and phenological characterization (Frison et al. 2018; Dubois et al. 2020) and detection of anomalies (Schellenberg et al. 2023).

Backscatter intensity is sensitive to vegetation moisture (Ezzahar et al. 2019), a triggering factor of fungi production (Ágreda et al. 2015). Processing easiness and intuitive interpretation make backscatter intensity the preferred feature in SAR-based time series analysis. At C-band, the VH backscatter intensity is more sensitive to volume, making the upper canopy response dominant in this polarization (Brown et al. 2003), whereas VV backscatter is more sensitive to texture and may respond to the vegetation-soil interplay (Velooso et al. 2017). Some atmospheric interferences may attenuate C-band SAR backscattering (Danklmayer et al. 2009), but rain may also increase SAR signal (Doblas et al. 2020), becoming these data useful to evaluate rain storage and soil moisture in forests (de Jong et al. 2000; Vaca and van der Tol 2018; Benninga et al. 2019).

Interferometric SAR (InSAR) exploits the phase difference between two complex SAR observations of the same area acquired from different sensor positions and extracts distance information about the Earth's terrain (Gens and Genderen 1996; Ferretti et al. 2000). Interferometry has been applied for land cover classification (Jacob et al. 2020; Rizzoli et al. 2022) and crop mapping and monitoring (Mestre-Quereda et al. 2020; Villarroya-Carpio et al. 2022). In a forestry context, the interferometric coherence parameter can be related to structure (Pinto et al. 2013), and the time series of this parameter have shown useful to detect changes (Mastro et al. 2022). The temporal decorrelation of repeat-pass InSAR is known to hinder some applications (Ahmed

et al. 2011), but it may facilitate the identification of triggering punctual phenomena like mushroom production.

Our goal is to explore the potential of time series C-band SAR data from Sentinel-1 to characterize mushroom yields at the plot level in Mediterranean forests. The specific objectives are (1) to construct time series of Sentinel-1 data over mushroom-productive pine plots and characterize the temporal patterns present and (2) to investigate the relationship between C-band SAR time series patterns and the weekly yields of ectomycorrhizal and saprotrophic mushrooms.

## Materials and Methods

### Study Area and Experimental Design

The study area, centered at coordinates 41.61 N,  $-2.54$  W, encompasses 17,000 ha of pine forests in Soria province, Spain (Fig. 1). These reforestations of *Pinus pinaster* Ait. also host *Quercus pyrenaica* Willd. resprouts. The area is relatively flat with an altitude in the range of 1000–1200 m. The climate is Continental Mediterranean with cool winters (average January temperature of 2 °C) and marked summer drought, with annual rainfall between 500 and 700 mm.

Seventeen permanent plots of 150 m<sup>2</sup> (5 × 30 m) have been established in this forest since 1997, with an external fence preventing harvesting and trampling. Plots are stratified to represent different forest structures (Fig. 1). The diameter and height of all trees within the plots were measured in 2020, and the volume of aboveground biomass was derived from TLS (Terrestrial Laser Scanner) measurements acquired in 2022 (Martínez-Rodrigo et al. 2022).

All edible fungi fruiting bodies (sporocarps) are sampled weekly during the main fruiting period, which corresponds to the autumn months of September–December. Sporocarps are collected, fresh-weighted, and identified to the species level (Ágreda et al. 2015). A database with values of annual mushroom production at the plot level records the yields, indicating species, number of individuals and biomass per species. We used a temporal subset (2018–2021) of this database and split the sample into ectomycorrhizal and saprotroph trophic guilds (Rinaldi et al. 2008) for a more detailed understanding of the relationship between SAR data and mushroom production.

### Sentinel-1 and Precipitation Data

Sentinel-1 is a dual-satellite mission under the Copernicus programme of the European Commission, developed and managed by the European Space Agency (ESA). The Sentinel-1A and -1B satellites are equipped with a C-band synthetic aperture radar (SAR) sensor, operating at frequency of 5.405 GHz (wavelength of 5.56 cm) and capable of VV + VH dual polarization (ESA - Sentinel 1 2022). This dual polarization allows Sentinel-1 to gather information in two channels: VV channel, where the sensor emits and receives vertically polarized signals, and VH channel, where it emits vertically and receives horizontally. The VH cross-polarized channel, being more sensitive to volume scattering, is particularly responsive to forest canopy properties compared to the co-polarized VV channel (Udali et al. 2021). The default acquisition mode for Sentinel-1 over land is Interferometric Wide swath (IW), which provides data with a spatial resolution of 5 × 20 m

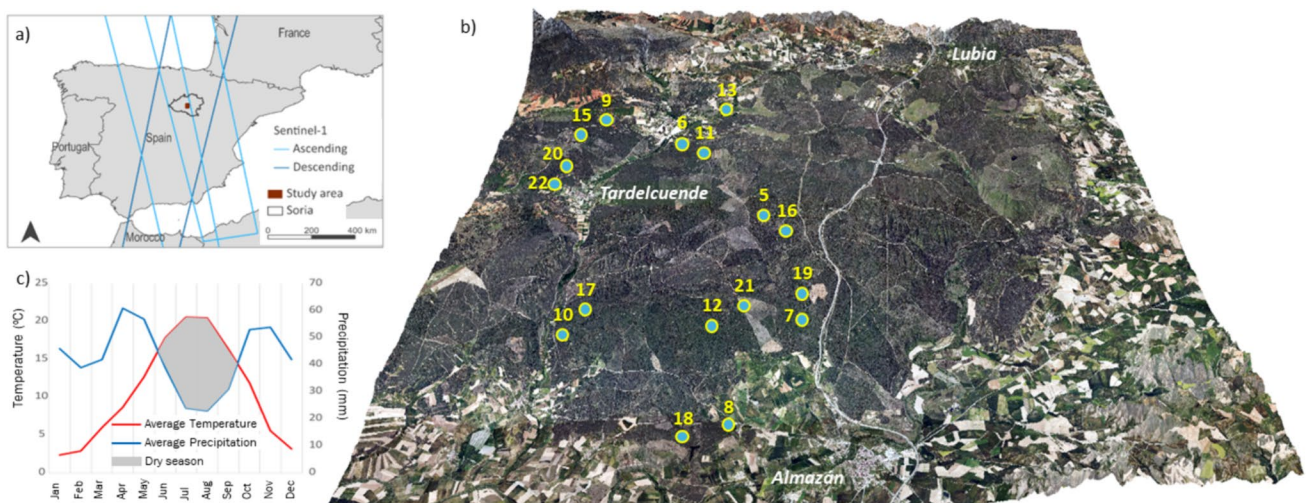


**Fig. 1** Study area. **a** Location in Spain and Sentinel-1 orbits; **b** arrangement of plots within the study area; and **c** climodiagram

and a nominal 6-day temporal resolution, assuming data from both satellites are utilized (Torres et al. 2012).

To analyze four complete years of time series data, we downloaded all accessible data acquired over the study area from January 5, 2018, to December 21, 2021. The power supply system failure in Sentinel-1B in December 2021 precluded further acquisitions from this satellite. Sentinel-1 data were downloaded from the Alaska Satellite Facility (ASF, <https://search.asf.alaska.edu/>).

Daily precipitation data were retrieved from the Spanish Meteorological Agency (AEMET, <http://www.aemet.es>) station in Soria.

### Analysis Workflow

The methodology in this study involves processing time series data from remote sensing and field measurements, imputing data to experimental plots, and performing statistical analysis of the time series data (Fig. 2).

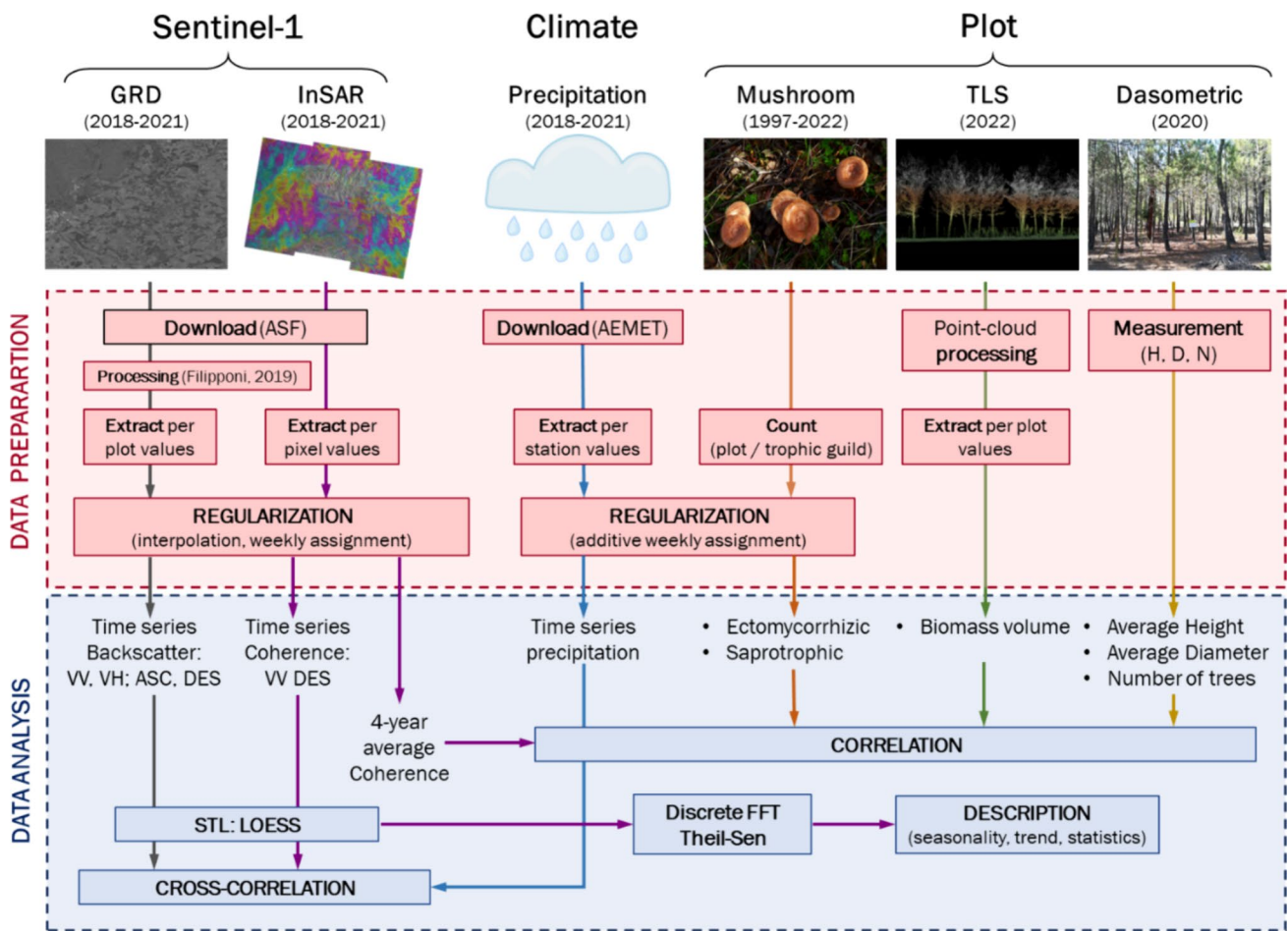


**Fig. 2** Schematic workflow of the main stages in the methodology for characterizing mushroom productive plots using time series Sentinel-1 SAR data

**Table 1** Summary of Sentinel-1 datasets downloaded and processed, indicating the number of dates required to image the entire study area

Orbit type	2018			2019			2020			2021			Total
	Asc	Des	Tot										
Slices downloaded and processed	128	151	279	114	107	221	151	148	299	152	125	277	1076
Data dates	97	61	158	85	58	143	120	59	179	120	57	177	657

## Backscatter Intensity Datasets

To derive time series of backscatter intensity, 1076 Sentinel-1 slices from ascending and descending orbits (Table 1) were downloaded in Ground Range Detected (GRD) mode. GRD products are multi-looked, projected to ground range using an Earth ellipsoid model (e.g., WGS84), and feature square pixels representing the intensity of the returned SAR pulse. These products were further processed using a standard workflow (Filipponi 2019) with the Sentinel-1 Toolbox in SNAP. Our processing included applying orbit file, thermal noise removal, calibration to radiometric backscatter, terrain flattening, speckle filter (Boxcar,  $5 \times 5$ ), range Doppler terrain correction, and linear to dB transformation. The resulting products are raster sets of backscatter intensity values corrected for local topography and various sources of noise, with  $10 \times 10$  m square pixels projected to WGS84 UTM30.

## Interferometric Coherence Datasets

Sentinel-1 Single Look Complex (SLC) data collected in Interferometric Wide-Swath (IW) mode include both amplitude and complex phase information. Interferometric techniques leverage this complex signal, comparing SAR observations acquired at different dates to measure their correlation, a parameter known as interferometric coherence, and which ranges from 0 to 1. Coherence values serve as indicators of landscape changes: low coherence indicate notable changes, while high coherence identifies stable scatterers.

Aggregating coherence values over time enables the identification of variability patterns across the landscape. Specifically, in interpreting time series of coherence over vegetation cover, a value of 0 indicates low correlation between consecutive acquisitions and suggests high variation over time, whereas a value of 1 indicates high correlation and little variation over time (Borlaf-Mena et al. 2021).

We ordered and downloaded 6-day interval VV-pol interferograms processed with HyP3 (Hogenson et al. 2020) from the ASF Data Search Vertex portal, to generate time series data. For InSAR pairs, we selected a  $10 \times 2$  multi-look size to achieve a 40-m pixel resolution.

We retrieved interferograms from 235 image pairs in descending orbit, spanning from January 5, 2018, to December 21, 2021. This regular series was only interrupted three times due to the absence of Sentinel-1 acquisitions (June 29, 2019, December 8, 2020, and August 11, 2021). Similarly, an equal number of interferometric pairs were available in ascending orbit, but we excluded them due to incomplete coverage of the study area.

## Retrieval of SAR and Precipitation Time Series

We retrieved time series of VV and VH backscatter intensity corresponding to the average value of pixels within the mushroom plots, along with VV interferometric coherence corresponding to the centroids of these plots. These time series were regularized to a 7-day frequency by averaging weekly values and interpolating missing data using a third-degree polynomial model. To enhance quality and reduce noise, we applied seasonal, trend, and remainder decomposition (STL, seasonal-trend decomposition using LOESS) (Cleveland et al. 1990). This method involves smoothing large residuals with a locally estimated scatterplot smoothing filter, rather than outright removal. The three STL components relate to the raw time series as follows (Eq. (1)):

$$Y_i = S_i + T_i + R_i \quad (1)$$

where  $Y_i$  = raw time series value at point  $i$ .  $S_i$  = time series seasonal component value at point  $i$ .  $T_i$  = time series trend component value at point  $i$ .  $R_i$  = time series remainder component value at point  $i$ . A similarly regular time series of precipitation was built with weekly accumulated values of rainfall.

## Characterization of Sentinel-1 Time Series

The denoised seasonal plus trend time series of SAR backscatter intensity and interferometric coherence for each plot were analyzed to identify variations on intra- and interannual scales. The presence and degree of trends were tested using the Theil-Sen estimator (Theil 1950; Sen 1968) which interprets the linear trend as the slope of the series (Chervenkov and Slavov 2019).

Seasonality in the interferometric coherence's seasonal component was analyzed via Fourier decomposition, which breaks down the time series into simpler functions (Hsu and Mehra 1987) using the Fast Fourier Transform (Brigham 1988). This transformation converts a signal into its sinusoidal components by decomposing any periodic signal into a sum of sinusoids, each harmonically related to the original signal's frequency (Semmlow 2012). The dominant frequencies were interpreted as indicators of cyclic patterns.

## Statistical Relationship Between SAR and Precipitation Time Series

To investigate the temporal relationship between SAR time series (backscatter intensity and interferometric coherence) and precipitation, we examined the cross correlation between these data sets on a weekly scale. The goal was to

determine whether an event in one time series (precipitation) triggers changes in the other (SAR) or they are independent (Brockwell and Davis 2016). If precipitation influences SAR values, this effect could be immediate or occur with some delay. For this analysis, we considered the average backscatter (VV and VH) and coherence values across all plots.

To explore the temporal relationship between interferometric coherence and mushroom yields, we analyzed the rate and direction of change in the temporal derivative of SAR interferometric coherence, following the method used by Gómez et al. (2011). The temporal derivative of interferometric coherence ( $D_{coh}$ ) was calculated as the difference in coherence values between consecutive dates, divided by the time interval between them, as shown in Eq. (2). We focused on the relationship between  $D_{coh}$  and the yearly first emergence of mushrooms in productive plots.

$$D_{coh} = \frac{(Co_{t+1} - Co_t)}{t} \quad (2)$$

## Results

### Characterization of Mushroom Productive Plots

Plots are structurally diverse (Fig. 3; Table 2) with 8.9–16.91 m average tree height and 16.23–42.58 cm average tree diameter. Plot 21 has the maximum number of trees with minimum average diameter, and plot 16 has the minimum number of trees with largest average diameter. Plot 15 has the tallest trees on average, and plot 20 the shortest. Plot 22 has the most volume biomass, and plot 18 is the least dense and with minimum volume biomass.

### Relationship Between Interferometric Coherence and Field Parameters

As shown in Fig. 4, despite the limited number of samples, we find a strong negative relationship between interferometric coherence and average tree height at the plot level ( $R = -0.70$ ), as well as between coherence and average tree diameter ( $R = -0.67$ ) within their respective ranges of 8–18 m for tree height and 0.16–0.42 m for tree diameter. Conversely, interferometric coherence shows a strong positive relationship with biomass volume per plot ( $R = 0.57$ ) and the number of trees per plot ( $R = 0.56$ ).

Figure 5 shows that the relationship between interferometric coherence and the average production of ectomycorrhizal mushrooms is moderately strong and positive ( $R = 0.47$ ). In contrast, the relationship with the average production of saprophytic mushrooms is weak and negative ( $R = -0.17$ ).

### Characterization of Sentinel-1 Backscatter Intensity Time Series

During the 4 years of data examined, Sentinel-1 co-pol (VV) backscatter intensity corresponding to mushroom plots was higher than cross-pol (VH) intensity in both descending (morning at 6 a.m.) and ascending (evening at 6 p.m.) orbits (Fig. 6).

Averaging the individual time series values per plot over the entire period, the lowest intensity values for both VH and VV were observed in plot 22 (the plot with the most biomass volume) in descending acquisitions and in plot 21 (the plot with the greatest number of trees) in ascending acquisitions. The highest values were recorded in plots 17 and 11 during morning orbits and in plots 8 and 19 during evening orbits.

The average dynamic ranges of VH and VV backscatter intensity values were 4.1 and 3.9 dB in ascending orbit and 2.9 and 3.4 dB in descending orbit. The maximum values were 5.9 dB in plots 12 and 22 (ascending) and 3.9 and 4.8 dB in plots 7 and 22 (descending).

The SAR intensity time series evaluated using the Theil-Sen slope do not show a significant overall trend. A statistical summary of trend values in the backscatter coefficient time series (Table 3) reveals that in the evening time series (ascending), most plots have a decreasing trend in both VH and VV polarizations. Conversely, in the morning time series (descending) most plots display an increasing trend over time. Additionally, the overall patterns of the intensity series are irregular and noisy, lacking any cyclic structure over the 4-year period considered.

### Characterization of Sentinel-1 Interferometric Coherence Time Series

Average interferometric coherence in descending orbit over the entire period ranged from 0.59 in plot 8 to 0.75 in plot 21. All coherence time series showed a positive trend with high slope values over time, as calculated with Theil-Sen test, ranging from 237 (plot 9) to 114.29 (plot 6). The highest increasing trends were observed in plots 9, 21, 18, and 7, while the lowest were in plots 6, 16, 15, and 11.

The coherence time series showed an annual periodic pattern in all plots, readily identifiable by visual inspection and complemented with individualized minor traits. The highest coherence values (0.76–0.98) were recorded in September and the lowest values (0.16–0.35) in January (Fig. 7). Fourier analysis demonstrated that, in addition to the annual frequency, most plots have 26-, 17- and 13-week frequency patterns, indicating cyclicity every 6, 3, and 2 months. However, plots 6 and 18 did not show the 13-week cyclicity and plot 8 lacked the 17-week cyclicity.

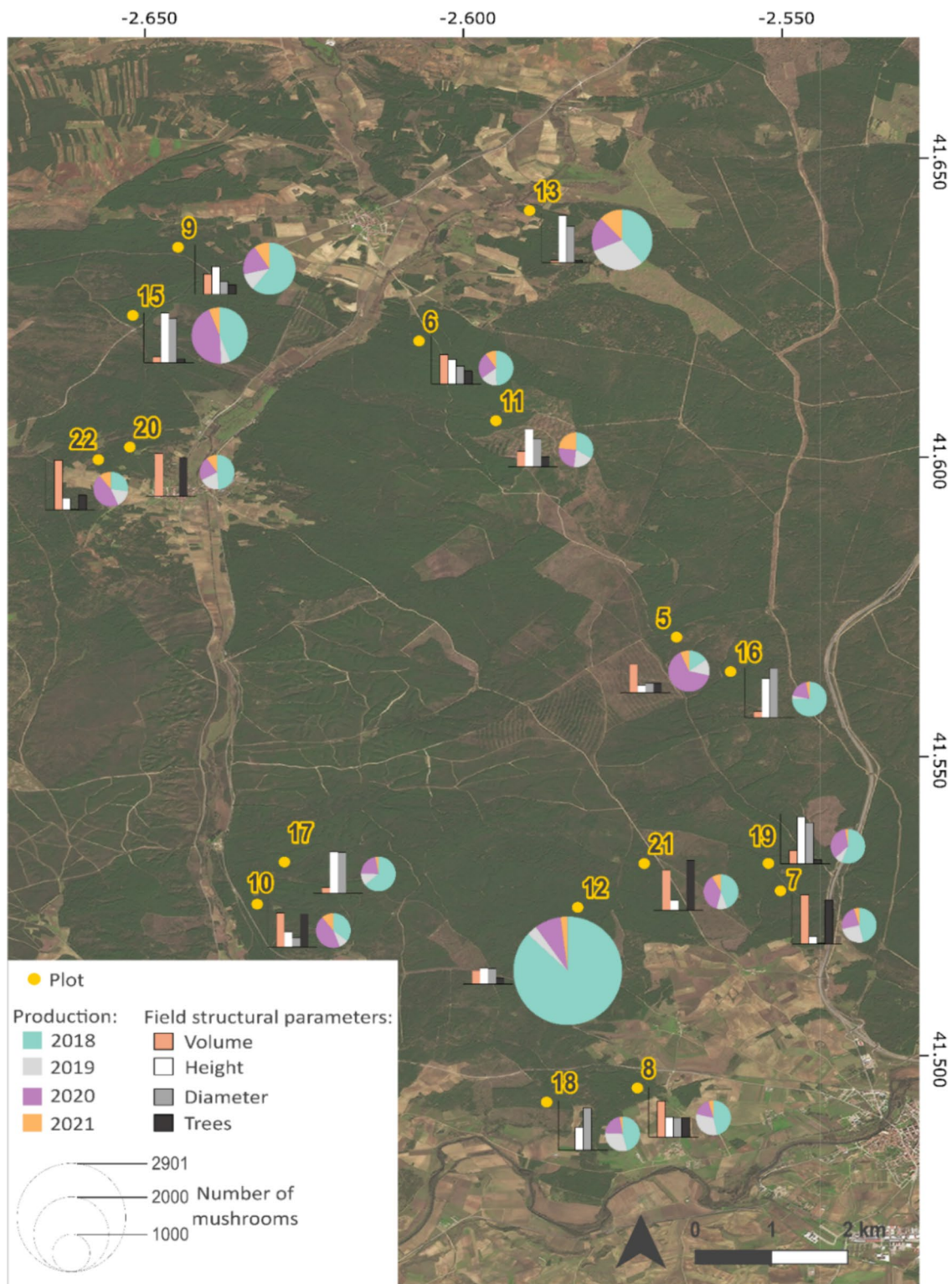


**Fig. 3** Spatial distribution of forest structural variability and mushroom productivity during the period 2018–2021

The amplitude in the Fourier decomposition represents the magnitude of each component function, with the annual periodicity (amplitude 10.72–22.46) being dominant over other less relevant periodicities (Table 4). Plot

17, which had the greatest number of trees, recorded the maximum amplitude in the 26-week frequency and plot 22 (with the maximum biomass volume) in the 13-week frequency.

**Table 2** Description of structural variables in mushroom productive plots

Variable	Max	Min	Mean	Stedv	Plot (max)	Plot (min)
Volume biomass (m <sup>3</sup> ha <sup>-1</sup> )	300.95	151.53	221.60	49.16	22	18
Average height (m)	16.91	8.90	12.94	2.57	15	20
Average diameter (cm)	42.58	16.23	27.71	9.34	16	21
Trees (#)	50.00	9.00	21.47	13.34	21	18, 17, and 16

**Fig. 4** Statistical relationship between interferometric coherence and forest structural variables

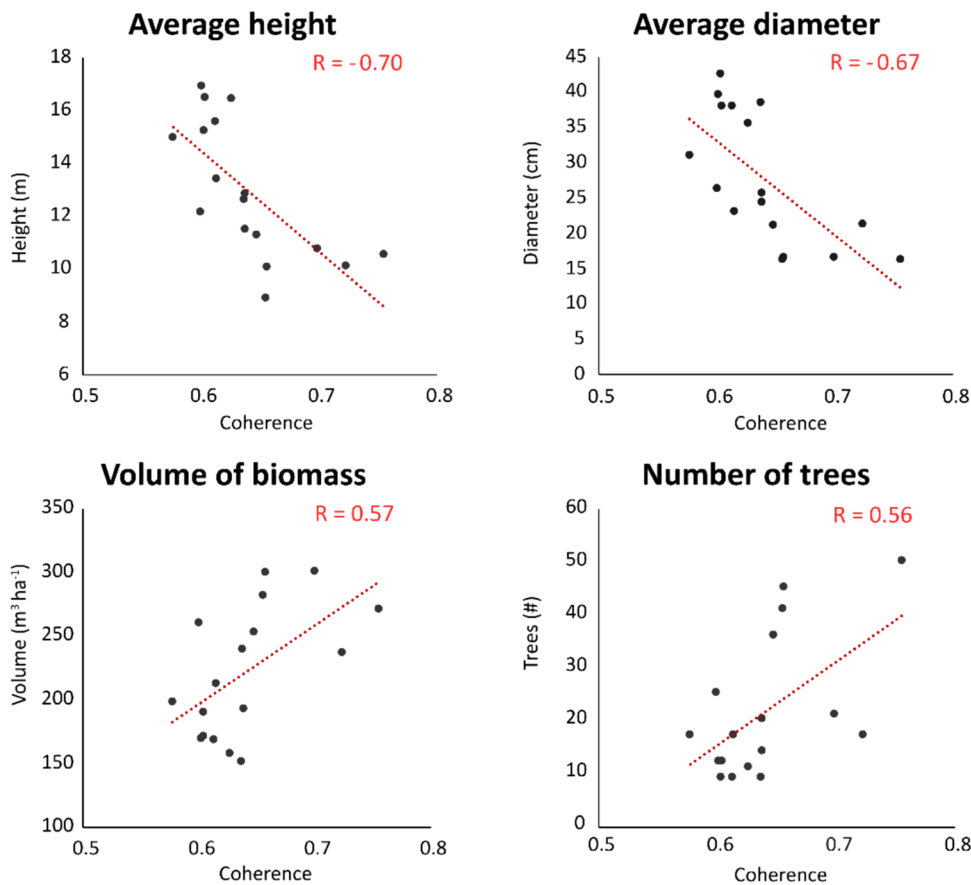


**Fig. 5** Statistical relationship between interferometric coherence and mushroom production

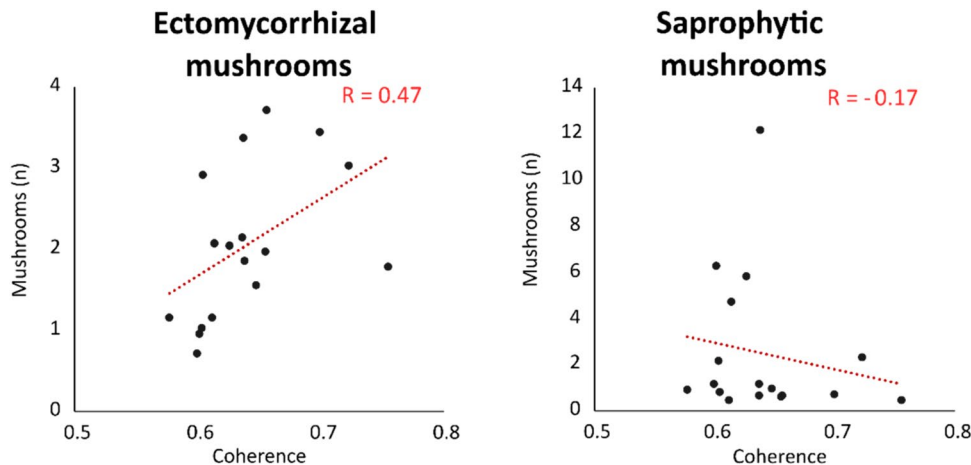


**Fig. 6** Average values of intensity per plot during the period considered (2018–2021), per polarization and orbit direction

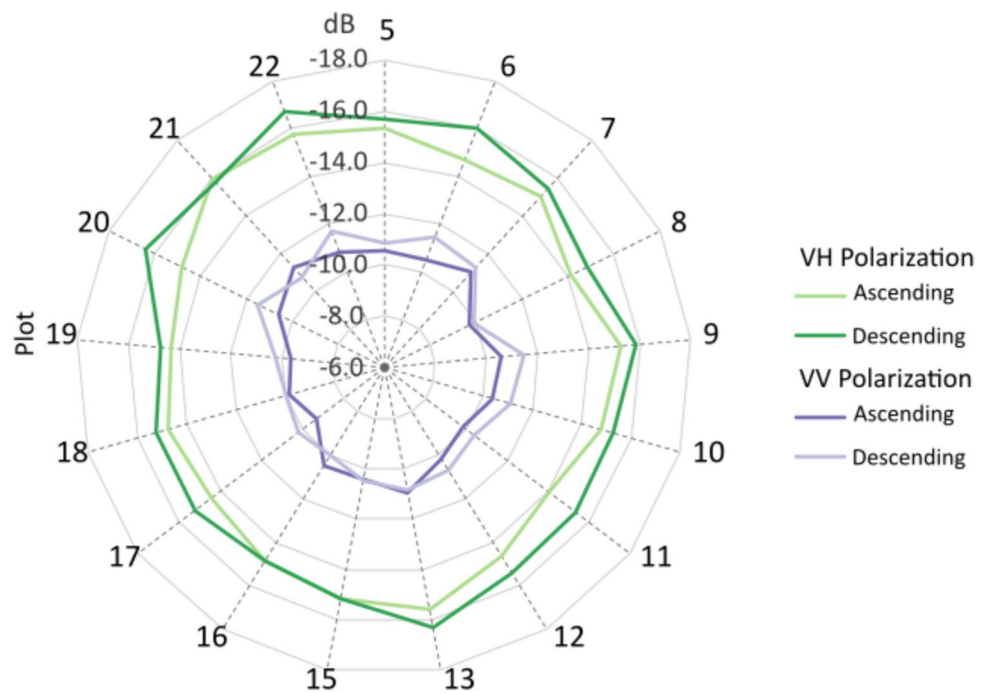


**Table 3** Statistical summary of Theil-Sen slope values for the time series of the backscatter coefficient

Orbit	Polarization	Plots		Range			Number of plots according to trend	
		Max trend	Min trend	Max	Min	Mean	Positive	Negative
Ascending	VV	22 and 7	16 and 9	12.39	-13.51	-3.05	5	12
	VH	15 and 9	18 and 8	12.62	-16.61	-0.72	8	9
Descending	VV	11 and 8	15 and 6	44.82	-46.59	5.61	11	6
	VH	15 and 11	5 and 13	35.5	-28.19	5.76	8	9

In most plots, mushroom production was triggered when coherence dropped drastically (Fig. 7). Most plots began producing ectomycorrhizal sporocarps 4 weeks after a peak in coherence transitioned to lower values (local minimum in the derivative values). Exceptions included plots 20, 16, and 17, where ectomycorrhizal production began a few weeks after the maximum change in coherence.

### Statistical Relationship Between SAR and Precipitation Time Series

Our analysis of the cross correlation between precipitation and SAR features time series reveals a statistically significant relationship (confidence level > 95%). This relationship is observed in both VH and VV polarizations for ascending and descending acquisitions. Notably, in ascending acquisitions, a significant correlation is evident at lag 0, indicating an immediate response to precipitation events (Fig. 8a, b). In contrast, descending acquisitions show a delayed correlation, with a notable

impact observed 2 to 3 weeks after precipitation (Fig. 8c, d). This suggests that precipitation affects backscatter values within this time frame. Interestingly, the correlation between precipitation and interferometric coherence does not manifest immediately in these forests. As shown in Fig. 9, the correlation values for interferometric coherence remain below the significance threshold.

### Discussion

Wild mushroom production is directly influenced by forest structure, climate, and terrain characteristics (Tomao et al. 2017). Among these factors, forest structure is the only one that can be managed through interventions such as adjusting species composition and basal area (Collado et al. 2020). Recently, an Aerial Laser Scanning (ALS)-based forest inventory was employed for tactical forest planning, utilizing clustered silvicultural treatments to promote mushroom yields (Pascual and de-Miguel 2022). This ALS-based

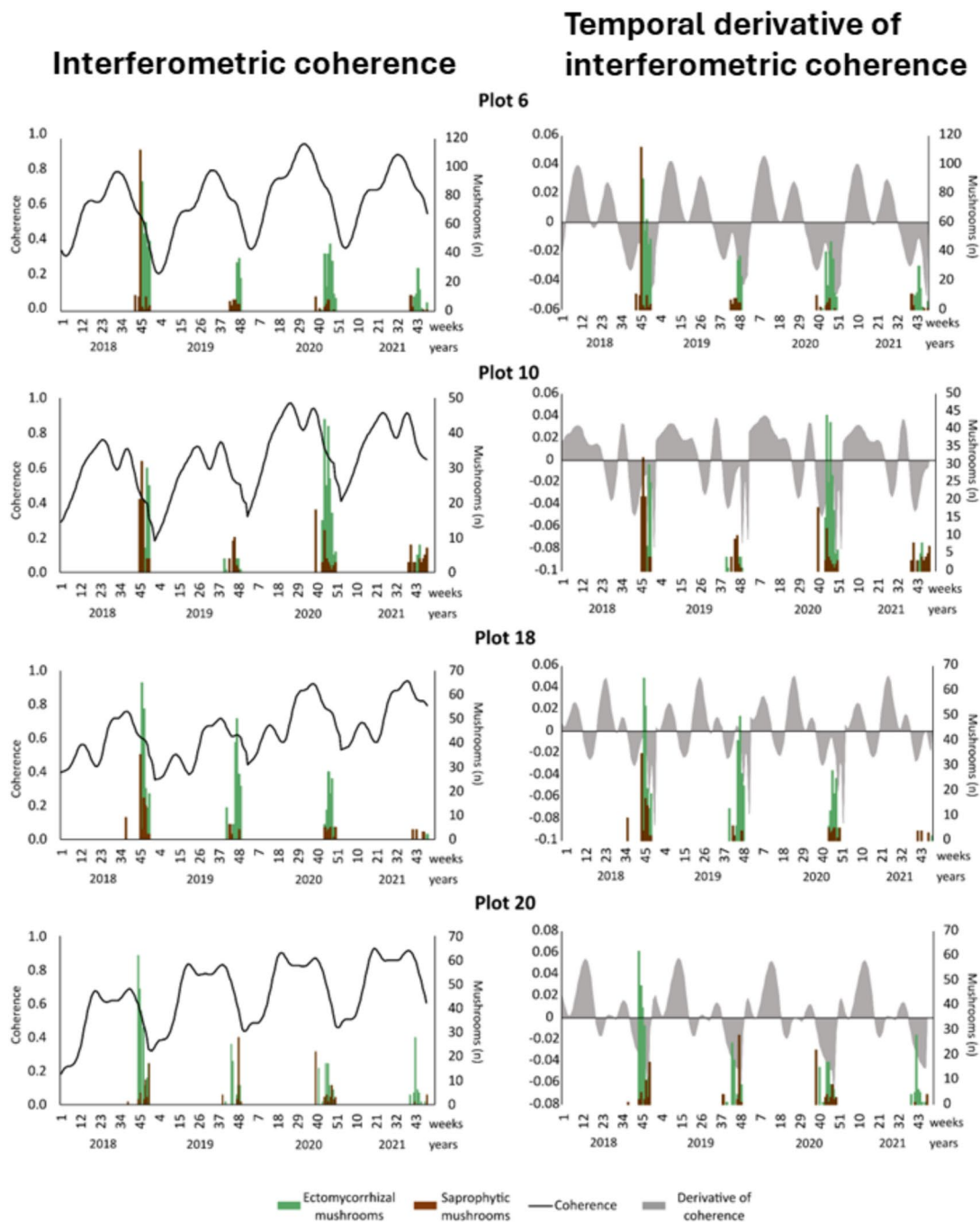


**Fig. 7** Examples of time series patterns of coherence and its temporal derivative in mushroom productive plots along with mushroom production

**Table 4** Summary of the Fourier amplitude statistics of coherence time series

Amplitude			
Period (days)	Max	Min	Mean
52	22.46 (plot 6)	10.72 (plot 21)	17.23
26	12.35 (plot 17)	3.66 (plot 13)	7.445
17	8.27 (plot 13)	2.15 (plot 11)	4.59
13	5.11 (plot 22)	1.53 (plot 9)	2.71

inventory could be further improved by integrating remotely sensed data from the ESA’s Copernicus programme, which would enhance spatial coverage and increase the frequency of inventory updates.

SAR data can independently characterize forest structure at the stand level (e.g., Gómez et al. 2021), but its synergy with optical data can offer additional benefits (e.g., Li et al. 2022), especially under cloudy conditions. While backscatter intensity is commonly used, interferometric techniques

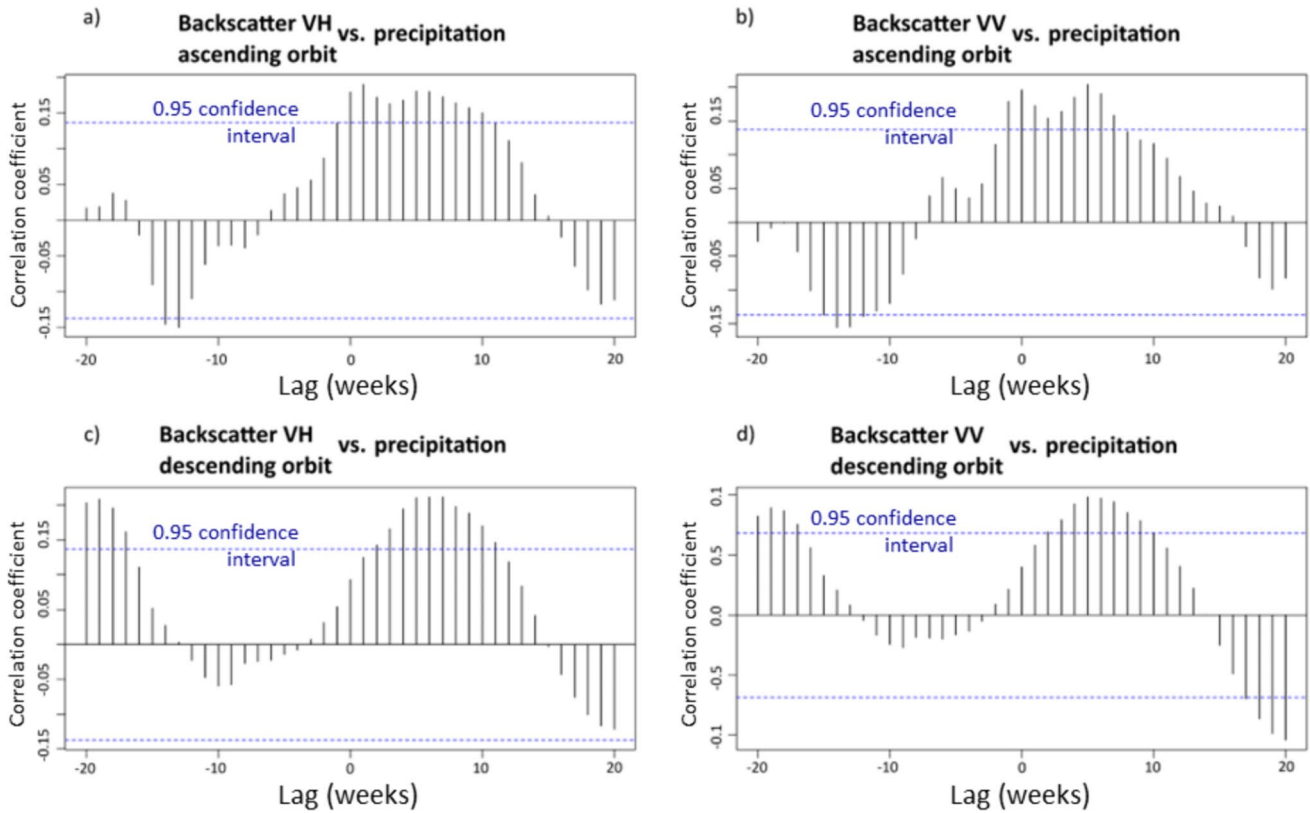
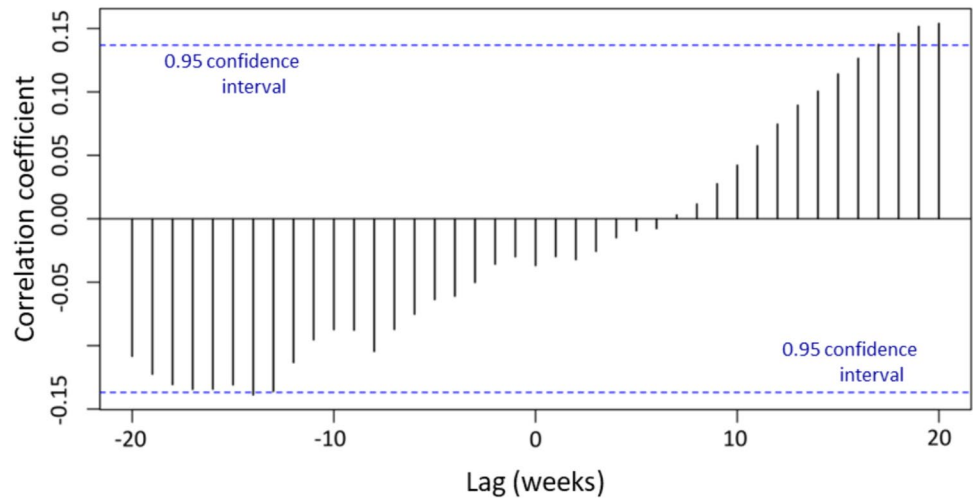


Fig. 8 Cross-correlation between backscatter intensity and precipitation

Fig. 9 Cross-correlation between interferometric coherence and precipitation

### Coherence vs. precipitation



present further opportunities by leveraging the scene stability between multiple data acquisitions. Therefore, Sentinel-1 interferometric coherence is increasingly being explored for various applications, such as monitoring grasslands (Abdel-Hamid et al. 2021) and detecting landslides (Ohki et al. 2020), thanks to the accessibility of data.

The short temporal interval enabled by the Sentinel-1 constellation is a critical factor for enhancing forest biomass and volume estimations (Cartus et al. 2022) and for monitoring changes and deforestation (Mastro et al. 2022) using time series of Sentinel-1 coherence. The advantage of a short temporal interval in coherence time series has also

been underscored by Seppi et al. (2022) who worked with L-band SAOCOM-1 in Argentinian forests. Our research, utilizing a 6-day revisit time of Sentinel-1 time series, contributes to this emerging field for characterizing wild mushroom productive plots and aiming to model their production.

In this work, we retrieved 4 years of weekly time series data from Sentinel-1, focusing on naturally productive mushroom plots in dry pine forests of Spain. Time series of backscatter intensity for both VH and VV polarizations were constructed, as well as VV interferometric coherence, to characterize seasonal variation patterns and relate them to weekly wild mushroom harvests from field surveys. We identified SAR time-series features that trigger autumn mushroom productivity in different plots.

Our results indicate that backscatter intensity is highly influenced by precipitation variability. Since precipitation triggers mushroom production (Ágreda et al. 2015), backscatter intensity and VH polarization values would appear useful for assessing this non-wood forest resource. However, in sparse and short Mediterranean forests, the C-band radar signal reaches the ground, strongly influencing backscatter intensity. Consequently, the backscatter time series become noisy, reducing its predictive power for mushroom yields.

High correlations were found between time-averaged values of coherence values and forest stand structure metrics, including mean plot height ( $R = -0.70$ ), mean tree diameter ( $R = -0.67$ ), plot volume ( $R = 0.57$ ), and number of trees ( $R = 0.56$ ), confirming that coherence is a good descriptor of forest structure. The relationship between interferometric coherence and mushroom production is stronger for ectomycorrhizal mushrooms than for saprotrophic mushrooms ( $R = 0.47$  versus  $R = -0.17$ ). Mycorrhizal species rely on carbon supplied by the host tree (Büntgen et al. 2011) for the production of sporocarps, while saprotrophic species acquire carbon from decomposition processes closely linked to soil moisture and temperature (Rousk and Bååth 2011). Thus, being more connected to the condition of the forest stand, mycorrhizal species production can be more effectively assessed with SAR data than saprotrophic species.

Time series of interferometric coherence measured with a 6-day interval in this forest scene are relatively stable and not influenced by punctual rainfall events, varying only with more persistent changes in local conditions. Therefore, coherence time-series could potentially indicate the drivers triggering mushroom production. The dynamic range of coherence values over time becomes key to exploiting the predicting capacity of the time series. A larger dynamic range of coherence suggests more transitional variations in the stand caused by environmental factors such as frost, persistent wind, and accumulated rainfall, which alter forest conditions. These disturbances also affect forest NDVI, driving annual spectrophenological patterns (Gómez et al. 2020). In this sense, Bai et al. (2020) demonstrated the

correlation between coherence amplitude and NDVI time series in monsoon forests of China, and Villarroya-Carpio et al. (2022) showed similar findings in agricultural crops of Spain. In our study area, mushroom production is directly linked to forest primary productivity as depicted by NDVI temporal curves (Olano et al. 2020).

Future work should explore the local relationship between NDVI and interferometric coherence time series to gain further insights into the potential and synergies of both parameters as indicators of the timing of fungal fruiting. Through a modest analysis relating the temporal derivative of coherence time series to the start of the mushroom season, we observed that changes in the forest — whether due to autumn instability caused by rainfall or wind — result in a marked decrease in coherence, which precedes mushroom production by approximately 4 weeks.

The availability of analysis ready data (ARD) facilitates complex analysis (Zhu 2019) for numerous applications. We accessed interferometric coherence from the ASF, simplifying SAR data processing but limiting analysis of non-standardly processed VV coherence. Other globally evaluated sources of interferometric coherence (Kellndorfer et al. 2022) enable potential characterization of forest structure for further applications. Self-processing of data provides flexibility in the parametrization and preparation, opening opportunities to explore combinations of indices (e.g., (Villarroya-Carpio and Lopez-Sanchez 2023)) that may complement explanations of vegetation temporal behavior.

The widespread availability and free access to high spatial and temporal resolution remotely sensed data are crucial for characterizing ecosystems and their components. There is an opportunity to contribute to the sustainable, efficient, and effective management of ecosystem functions, including predicting and quantifying non-wood forest products such as wild mushroom yields.

## Conclusions

This study highlights the potential of synthetic aperture radar (SAR) data, particularly from Sentinel-1, in enhancing the estimation and prediction of wild mushroom production in Mediterranean forests. Our findings demonstrate that backscatter intensity correlates strongly with precipitation and its noisy time series complicate interpretation. In contrast, the time series of interference coherence emerges as a valuable indicator for identifying the environmental conditions that trigger wild mushroom production.

To refine and improve predictive models for mushroom yields, future research should focus on integrating additional field data and considering a broader range of forest conditions. Exploring alternative SAR-based techniques and combining them with optical data could enhance the

accuracy and reliability of these models. This comprehensive approach will deepen our understanding of the factors influencing mushroom production and contribute to the sustainability management of non-wood forest products.

By leveraging high-resolution, frequently updated remote sensing data, we can develop more effective tools for forest management. These tools will not only help in predicting and quantifying mushroom yields but also aid in making informed decisions to support the conservation and sustainable use of forest resources. Overall, the advancements in SAR technology offer promising avenues for ecological research and the management of forest ecosystems.

**Acknowledgements** Consejería de Medio Ambiente de la Junta de Castilla y León maintains the network of wild mushroom productive plots and provides the data. Valonsadero Forestry Centre and CeseFor Foundation staff is thanked for their work collecting mushroom data. R. M-R. was working for Föra Forest Technologies when this work was performed.

**Funding** Open Access funding provided thanks to the CRUE-CSIC agreement with Springer Nature. This work was supported by the Spanish Ministry of Science and Innovation, under grant DI-17-9626, PID2020-117303 GB-C22/AEI/<https://doi.org/10.13039/501100011033> and by Cátedra CeI of Caja Rural de Soria.

#### Declarations

This work complies with all applicable ethical standards.

**Ethics Approval** This paper does not contain any studies with human participants or animals performed by any of the authors.

**Informed Consent** Informed consent was obtained from all the individual participants included in the study.

**Conflict of Interest** The authors declare no competing interests.

**Open Access** This article is licensed under a Creative Commons Attribution 4.0 International License, which permits use, sharing, adaptation, distribution and reproduction in any medium or format, as long as you give appropriate credit to the original author(s) and the source, provide a link to the Creative Commons licence, and indicate if changes were made. The images or other third party material in this article are included in the article's Creative Commons licence, unless indicated otherwise in a credit line to the material. If material is not included in the article's Creative Commons licence and your intended use is not permitted by statutory regulation or exceeds the permitted use, you will need to obtain permission directly from the copyright holder. To view a copy of this licence, visit <http://creativecommons.org/licenses/by/4.0/>.

## References

- Abdel-Hamid A, Dubovyk O, Greve K (2021) The potential of Sentinel-1 InSAR coherence for grasslands monitoring in Eastern Cape, South Africa. *Int J Appl Earth Obs Geoinf* 98:102306. <https://doi.org/10.1016/j.jag.2021.102306>
- Ágreda T, Cisneros Ó, Águeda B, Marina Fernández-Toirán L (2013) Age class influence on the yield of edible fungi in a managed Mediterranean forest. *Mycorrhiza*. <https://doi.org/10.1007/s00572-013-0522-y>
- Ágreda T, Águeda B, Olano JM et al (2015) Increased evapotranspiration demand in a Mediterranean climate might cause a decline in fungal yields under global warming. *Global Change Biology* 21. <https://doi.org/10.1111/gcb.12960>
- Ahmed R, Siqueira P, Hensley S et al (2011) A survey of temporal decorrelation from spaceborne L-Band repeat-pass InSAR. *Remote Sens Environ* 115:2887–2896. <https://doi.org/10.1016/j.rse.2010.03.017>
- Alday JG, Martínez De Aragón J, De-Miguel S, Bonet JA (2017) Mushroom biomass and diversity are driven by different spatio-temporal scales along Mediterranean elevation gradients. *Sci Rep* 7:45824. <https://doi.org/10.1038/srep45824>
- Bai Z, Fang S, Gao J et al (2020) Could vegetation index be derive from synthetic aperture radar? – The linear relationship between interferometric coherence and NDVI. *Sci Rep* 10:6749. <https://doi.org/10.1038/s41598-020-63560-0>
- Ballère M, Bouvet A, Mermoz S et al (2021) SAR data for tropical forest disturbance alerts in French Guiana: benefit over optical imagery. *Remote Sens Environ* 252:112159. <https://doi.org/10.1016/j.rse.2020.112159>
- Beland M, Sparrow B, Harding D et al (2019) On promoting the use of lidar systems in forest ecosystem research. *For Ecol Manage* 450:117484. <https://doi.org/10.1016/j.foreco.2019.117484>
- Benninga H-JF, van der Velde R, Su Z (2019) Impacts of radiometric uncertainty and weather-related surface conditions on soil moisture retrievals with Sentinel-1. *Remote Sens* 11:2025. <https://doi.org/10.3390/rs11172025>
- Blázquez-Casado Á, Calama R, Valbuena M et al (2019) Combining low-density LiDAR and satellite images to discriminate species in mixed Mediterranean forest. *Ann For Sci* 76:57. <https://doi.org/10.1007/s13595-019-0835-x>
- Borlaf-Mena I, Badea O, Tanase MA (2021) Assessing the utility of Sentinel-1 coherence time series for temperate and tropical forest mapping. *Remote Sens* 13:4814. <https://doi.org/10.3390/rs13234814>
- Brigham EO (1988) *The fast Fourier transform and its applications*. Prentice Hall, Englewood Cliffs
- Brockwell PJ, Davis RA (2016) *Introduction to time series and forecasting*. Springer International Publishing, Cham
- Brown SCM, Quegan S, Morrison K et al (2003) High-resolution measurements of scattering in wheat canopies-implications for crop parameter retrieval. *IEEE Trans Geosci Remote Sens* 41:1602–1610. <https://doi.org/10.1109/TGRS.2003.814132>
- Büntgen U, Tegel W, Egli S et al (2011) Truffles and climate change. *Front Ecol Environ* 9:150–151. <https://doi.org/10.1890/11.WB.004>
- Cartus O, Santoro M, Wegmuller U et al (2022) Sentinel-1 coherence for mapping above-ground biomass in semiarid forest areas. *IEEE Geosci Remote Sens Lett* 19:1–5. <https://doi.org/10.1109/LGRS.2021.3071949>
- Chervenkov H, Slavov K (2019) Theil–Sen estimator vs. ordinary least squares — trend analysis for selected ETCCDI climate indices. “Prof. Marin Drinov” Publishing House of Bulgarian Academy of Sciences. <https://doi.org/10.7546/crabs.2019.01.06>
- Cleveland RB, Cleveland WS, McRae JE, Terpenning I (1990) STL: a seasonal-trend decomposition procedure based on loess. *J Off Stat* 6:3–73
- Cockle KL, Martin K, Robledo G (2012) Linking fungi, trees, and hole-using birds in a neotropical tree-cavity network: pathways of cavity production and implications for conservation. *For Ecol Manage* 264:210–219. <https://doi.org/10.1016/J.FORECO.2011.10.015>
- Collado E, Castaño C, Bonet JA et al (2020) Divergent above- and below-ground responses of fungal functional groups to forest

- thinning. *Soil Biol Biochem* 150:108010. <https://doi.org/10.1016/j.soilbio.2020.108010>
- Danklmayer A, Döring BJ, Schwerdt M, Chandra M (2009) Assessment of atmospheric propagation effects in SAR images. *IEEE Trans Geosci Remote Sens* 47:10. <https://doi.org/10.1109/TGRS.2009.2022271>
- Dassot M, Constant T, Fournier M (2011) The use of terrestrial LiDAR technology in forest science: application fields, benefits and challenges. *Ann For Sci* 68:959–974. <https://doi.org/10.1007/s13595-011-0102-2>
- de Jong J, Klaassen W, Ballast A (2000) Rain storage in forests detected with ERS tandem mission SAR. *Remote Sens Environ* 72:170–180. [https://doi.org/10.1016/S0034-4257\(99\)00100-5](https://doi.org/10.1016/S0034-4257(99)00100-5)
- Devkota S, Fang W, Arunachalam K et al (2023) Systematic review of fungi, their diversity and role in ecosystem services from the Far Eastern Himalayan Landscape (FHL). *Heliyon* 9:e12756. <https://doi.org/10.1016/j.heliyon.2022.e12756>
- Doblas J, Carneiro A, Shimabukuro Y et al (2020) Assessment of rainfall influence on Sentinel-1 time series on Amazonian tropical forests aiming deforestation detection improvement. In: 2020 IEEE Latin American GRSS & ISPRS Remote Sensing Conference (LAGIRS). pp 397–402
- Dostálová A, Wagner W, Milenković M, Hollaus M (2018) Annual seasonality in Sentinel-1 signal for forest mapping and forest type classification. *Int J Remote Sens* 39:7738–7760. <https://doi.org/10.1080/01431161.2018.1479788>
- Dubois C, Mueller MM, Pathe C et al (2020) Characterization of land cover seasonality in Sentinel-1 time series data. *ISPRS Ann Photogramm Remote Sens Spat Inf Sci V-3-2020:97–104*. <https://doi.org/10.5194/isprs-annals-V-3-2020-97-2020>
- Eitel JUH, Griffin KL, Boelman NT et al (2020) Remote sensing tracks daily radial wood growth of evergreen needleleaf trees. *Glob Change Biol* 26:4068–4078. <https://doi.org/10.1111/gcb.15112>
- ESA - Sentinel 1 (2022) Sentinel-1 - missions - sentinel online. <https://sentinel.esa.int/web/sentinel/missions/sentinel-1>. Accessed 18 Nov 2022
- Ezzahar J, Ouadi N, Zribi M et al (2019) Evaluation of backscattering models and support vector machine for the retrieval of bare soil moisture from Sentinel-1 data. *Remote Sensing* 12:72. <https://doi.org/10.3390/rs12010072>
- Ferretti A, Prati C, Rocca F (2000) Nonlinear subsidence rate estimation using permanent scatterers in differential SAR interferometry. *IEEE Trans Geosci Remote Sens* 38:2202–2212. <https://doi.org/10.1109/36.868878>
- Filipponi F (2019) Sentinel-1 GRD preprocessing workflow. In: 3rd International Electronic Conference on Remote Sensing. MDPI, p 11
- Frison P-L, Fruneau B, Kmiha S et al (2018) Potential of Sentinel-1 data for monitoring temperate mixed forest phenology. *Remote Sensing* 10:2049. <https://doi.org/10.3390/rs10122049>
- Gens R, Genderen JLV (1996) Review article SAR interferometry—issues, techniques, applications. *Int J Remote Sens* 17:1803–1835. <https://doi.org/10.1080/01431169608948741>
- Gómez C, White JC, Wulder MA (2011) Characterizing the state and processes of change in a dynamic forest environment using hierarchical spatio-temporal segmentation. *Remote Sens Environ* 115:1665–1679. <https://doi.org/10.1016/j.rse.2011.02.025>
- Gómez C, Lopez-Sanchez JM, Romero-Puig N et al (2021) Canopy height estimation in Mediterranean forests of Spain with TanDEM-X data. *IEEE J Sel Top Appl Earth Obs Remote Sens* 14:2956–2970. <https://doi.org/10.1109/JSTARS.2021.3060691>
- Gómez C, Alejandro P, Montes F (2020) Phenological characterization of *Fagus sylvatica* L. In: Mediterranean populations of the Spanish Central Range with Landsat OLI/ETM+ and Sentinel-2A/B. *Revista de Teledetección* 55:71–80. <https://doi.org/10.4995/raet.2020.13561>
- Herrero C, Berraondo I, Bravo F et al (2019) Predicting mushroom productivity from long-term field-data series in Mediterranean *Pinus pinaster* ait. forests in the context of climate change. *Forests* 10. <https://doi.org/10.3390/f10030206>
- Hogenson K, Arko SA, Büchler B et al (2016) Hybrid pluggable processing pipeline (HyP3): a cloud-based infrastructure for generic processing of SAR data
- Hsu HP, Mehra R (1987) *Análisis de Fourier*. Addison-Wesley Iberoamericana, México
- Indirabai I, Nair MVH, Nair JR et al (2019) Estimation of forest structural attributes using ICESat/GLAS-Spaceborne laser altimetry data in the Western Ghats Region of India. *J Geovis Spat Anal* 3:10. <https://doi.org/10.1007/s41651-019-0033-2>
- Jacob AW, Vicente-Guijalba F, Lopez-Martinez C et al (2020) Sentinel-1 InSAR coherence for land cover mapping: a comparison of multiple feature-based classifiers. *IEEE J Sel Top Appl Earth Obs Remote Sens* 13:535–552. <https://doi.org/10.1109/JSTARS.2019.2958847>
- Kellndorfer J, Cartus O, Lavallo M et al (2022) Global seasonal Sentinel-1 interferometric coherence and backscatter data set. *Sci Data* 9:73. <https://doi.org/10.1038/s41597-022-01189-6>
- Komisarenko V, Voormansik K, Elshawi R, Sakr S (2022) Exploiting time series of Sentinel-1 and Sentinel-2 to detect grassland mowing events using deep learning with reject region. *Sci Rep* 12:983. <https://doi.org/10.1038/s41598-022-04932-6>
- Küçüker DM, Başkent EZ (2014) Spatial prediction of *Lactarius deliciosus* and *Lactarius salmonicolor* mushroom distribution with logistic regression models in the Kızılcasu Planning Unit, Turkey. *Mycorrhiza* 25:1–11. <https://doi.org/10.1007/s00572-014-0583-6>
- Li X, Ye Z, Long J et al (2022) Inversion of Coniferous forest stock volume based on backscatter and InSAR coherence factors of Sentinel-1 hyper-temporal images and spectral variables of Landsat 8 OLI. *Remote Sensing* 14:2754. <https://doi.org/10.3390/rs14122754>
- Li J, Roy DP (2017) A global analysis of Sentinel-2a, Sentinel-2b and Landsat-8 data revisit intervals and implications for terrestrial monitoring. *Remote Sens* 9. <https://doi.org/10.3390/rs9090902>
- Martínez-Rodrigo R, Gómez C, Torano-Caicoya A et al (2022) Stand structural characteristics derived from combined TLS and Landsat data support predictions of mushroom yields in Mediterranean forest. *Remote Sensing* 14:5025. <https://doi.org/10.3390/rs14195025>
- Mastro P, Masiello G, Serio C, Pepe A (2022) Change interferometric coherence and backscatter for crop-type mapping and Sentinel-1 observations. *Remote Sensing* 14:3323. <https://doi.org/10.3390/rs14143323>
- Mestre-Quereda A, Lopez-Sanchez JM, Vicente-Guijalba F et al (2020) Time-series of Sentinel-1 interferometric coherence and backscatter for crop-type mapping. *IEEE J Sel Top Appl Earth Obs Remote Sens* 13:4070–4084. <https://doi.org/10.1109/JSTARS.2020.3008096>
- Müller J, Büttler R (2010) A review of habitat thresholds for dead wood: a baseline for management recommendations in European forests. *Eur J Forest Res* 129:981–992. <https://doi.org/10.1007/s10342-010-0400-5>
- Neumann M, Ferro-Famil L, Reigber A (2010) Estimation of forest structure, ground, and canopy layer characteristics from multi-baseline polarimetric interferometric SAR data. *IEEE Trans Geosci Remote Sens* 48:1086–1104. <https://doi.org/10.1109/TGRS.2009.2031101>
- Ohki M, Abe T, Tadono T, Shimada M (2020) Landslide detection in mountainous forest areas using polarimetry and interferometric coherence. *Earth Planets Space* 72:67. <https://doi.org/10.1186/s40623-020-01191-5>

- Olano JM, Martínez-Rodrigo R, Altelaarrea JM et al (2020) Primary productivity and climate control mushroom yields in Mediterranean pine forests. *Agric For Meteorol*. <https://doi.org/10.1016/j.agrformet.2020.108015>
- Pascual A, de-Miguel S (2022) Evaluation of mushroom production potential by combining spatial optimization and LiDAR-based forest mapping data. *Sci Total Environ* 850:157980. <https://doi.org/10.1016/j.scitotenv.2022.157980>
- Pinto N, Simard M, Dubayah R (2013) Using InSAR coherence to map stand age in a boreal forest. *Remote Sens* 5:42–56. <https://doi.org/10.3390/rs5010042>
- Pullella A, Araújo Santos R, Sica F et al (2020) Multi-temporal Sentinel-1 backscatter and coherence for rainforest mapping. *Remote Sens* 12:847. <https://doi.org/10.3390/rs12050847>
- Rinaldi AC, Comandini O, Kuyper TW (2008) Ectomycorrhizal fungal diversity: separating the wheat from the chaff. *Fungal Divers* 33:1–45
- Rizzoli P, Dell'Amore L, Bueso-Bello J-L et al (2022) On the derivation of volume decorrelation from TanDEM-X bistatic coherence. *IEEE J Sel Top Appl Earth Obs Remote Sens* 15:3504–3518. <https://doi.org/10.1109/JSTARS.2022.3170076>
- Rousk J, Bååth E (2011) Growth of saprotrophic fungi and bacteria in soil: growth of saprotrophic fungi and bacteria in soil. *FEMS Microbiol Ecol* 78:17–30. <https://doi.org/10.1111/j.1574-6941.2011.01106.x>
- Rubio-Cuadrado Á, Camarero JJ, Rodríguez-Calcerrada J et al (2021) Impact of successive spring frosts on leaf phenology and radial growth in three deciduous tree species with contrasting climate requirements in central Spain. *Tree Physiol* 41:2279–2292. <https://doi.org/10.1093/treephys/tpab076>
- Schellenberg K, Jagdhuber T, Zehner M et al (2023) Potential of Sentinel-1 SAR to assess damage in drought-affected temperate deciduous broadleaf forests. *Remote Sens* 15:1004. <https://doi.org/10.3390/rs15041004>
- Semmlow J (2012) Chapter 3- Fourier transform: introduction. In: Semmlow J (ed) *Signals and systems for bioengineers*, 2nd edn. Academic Press, Boston, pp 81–129
- Sen PK (1968) Estimates of the regression coefficient based on Kendall's tau. *J Am Stat Assoc* 63:1379–1389. <https://doi.org/10.1080/01621459.1968.10480934>
- Seppi SA, López-Martínez C, Joseau MJ (2022) Assessment of L-Band SAOCOM InSAR coherence and its comparison with C-Band: a case study over managed forests in Argentina. *Remote Sens* 14:5652. <https://doi.org/10.3390/rs14225652>
- Soares C, Silva JMN, Boavida-Portugal J, Cerasoli S (2022) Spectral-based monitoring of climate effects on the inter-annual variability of different plant functional types in Mediterranean Cork Oak Woodlands. *Remote Sens* 14:711. <https://doi.org/10.3390/rs14030711>
- Tanase MA, Villard L, Pitar D et al (2019) Synthetic aperture radar sensitivity to forest changes: a simulations-based study for the Romanian forests. *Sci Total Environ* 689:1104–1114. <https://doi.org/10.1016/j.scitotenv.2019.06.494>
- Theil H (1950) A rank-invariant method of linear and polynomial regression analysis, I and II. Reprinted from *Indag Math XII* (2)
- Tomao A, Bonet JA, Martínez de Aragón J, de-Miguel S (2017) Is silviculture able to enhance wild forest mushroom resources? Current knowledge and future perspectives. *For Ecol Manage* 402:102–114. <https://doi.org/10.1016/j.foreco.2017.07.039>
- Torres R, Snoeij P, Geudtner D et al (2012) GMES Sentinel-1 mission. *Remote Sens Environ* 120:9–24. <https://doi.org/10.1016/j.rse.2011.05.028>
- Udali A, Lingua E, Persson HJ (2021) Assessing forest type and tree species classification using Sentinel-1 C-Band SAR data in Southern Sweden. *Remote Sensing* 13:3237. <https://doi.org/10.3390/rs13163237>
- Vaca CC, van der Tol C (2018) Sensitivity of Sentinel-1 to rain stored in temperate forest. In: *IGARSS 2018 - 2018 IEEE International Geoscience and Remote Sensing Symposium*. pp 5330–5333
- Veloso A, Mermoz S, Bouvet A et al (2017) Understanding the temporal behavior of crops using Sentinel-1 and Sentinel-2-like data for agricultural applications. *Remote Sens Environ* 199:415–426. <https://doi.org/10.1016/j.rse.2017.07.015>
- Villarroya-Carpio A, Lopez-Sanchez JM (2023) Multi-annual evaluation of time series of Sentinel-1 interferometric coherence as a tool for crop monitoring. *Sensors* 23:1833. <https://doi.org/10.3390/s23041833>
- Villarroya-Carpio A, Lopez-Sanchez JM, Engdahl ME (2022) Sentinel-1 interferometric coherence as a vegetation index for agriculture. *Remote Sens Environ* 280:113208. <https://doi.org/10.1016/j.rse.2022.113208>
- White JC, Coops NC, Wulder MA et al (2016) Remote sensing technologies for enhancing forest inventories: a review. *Can J Remote Sens* 42:619–641. <https://doi.org/10.1080/07038992.2016.1207484>
- Zhu Z (2019) Science of landsat analysis ready data. *Remote Sensing* 11:2166. <https://doi.org/10.3390/rs11182166>

**Publisher's Note** Springer Nature remains neutral with regard to jurisdictional claims in published maps and institutional affiliations.